Tuberculosis 146 (2024) 102494

Contents lists available at ScienceDirect

Tuberculosis

journal homepage: www.elsevier.com/locate/tube

Demonstrating the utility of the *ex vivo* murine mycobacterial growth inhibition assay (MGIA) for high-throughput screening of tuberculosis vaccine candidates against multiple *Mycobacterium tuberculosis* complex strains

Hannah Painter [a,*], Sam Willcocks [a,1], Andrea Zelmer [a], Rajko Reljic [b], Rachel Tanner [c], Helen Fletcher [a]

[a] Department of Infection Biology, London School of Hygiene and Tropical Medicine, Keppel Street, London, WC1E 7HT, UK
[b] Institute of Infection and Immunity, St George's University of London, Cranmer Terrrace, London, SW17 0RE, UK
[c] Department of Biology, University of Oxford, Old Road Campus Research Building, Roosevelt Drive, Oxford, OX3 7DQ, UK

ARTICLE INFO

Keywords:
Mycobacterial growth inhibition assay
Tuberculosis
Vaccines
3Rs
Mouse

ABSTRACT

Human tuberculosis (TB) is caused by various members of the *Mycobacterium tuberculosis* (Mtb) complex. Differences in host response to infection have been reported, illustrative of a need to evaluate efficacy of novel vaccine candidates against multiple strains in preclinical studies. We previously showed that the murine lung and spleen direct mycobacterial growth inhibition assay (MGIA) can be used to assess control of *ex vivo* mycobacterial growth by host cells. The number of mice required for the assay is significantly lower than *in vivo* studies, facilitating testing of multiple strains and/or the incorporation of other cellular analyses. Here, we provide proof-of-concept that the murine MGIA can be applied to evaluate vaccine-induced protection against multiple Mtb clinical isolates. Using an ancient and modern strain of the Mtb complex, we demonstrate that *ex vivo* bacillus Calmette–Guérin (BCG)-mediated mycobacterial growth inhibition recapitulates protection observed in the lung and spleen following *in vivo* infection of mice. Further, we provide the first report of cellular and transcriptional correlates of BCG-induced growth inhibition in the lung MGIA. The *ex vivo* MGIA represents a promising platform to gain early insight into vaccine performance against a collection of Mtb strains and improve preclinical evaluation of TB vaccine candidates.

1. Introduction

Human tuberculosis (TB), caused by bacteria from the *Mycobacterium tuberculosis* (Mtb) complex, remains a major global health concern [1]. A vaccine able to sufficiently control the global TB crisis is currently unavailable. One challenging aspect that hampers TB vaccine research and development efforts is the difficulty in translating preclinical candidates into the clinic [2]. Disease presentation and the immune response to infection and vaccination varies between humans and animal models. Further, the conditions of experimental challenge together with dose, frequency and strain of Mtb used also fail to mimic natural exposure [2,3]. Particular strains belonging to specific Mtb complex species and Mtb lineages display pronounced differences, and in the clinical setting, strains differ geographically and may also exhibit drug resistance [4]. It is critical that novel TB vaccine candidates demonstrate protection against circulating Mtb strains of clinical relevance. However, ability to screen vaccine efficacy against a range of Mtb strains in preclinical models is limited as each strain doubles the number of experimental groups required, posing logistical and ethical challenges.

Advances in whole-genome sequencing have facilitated the study of large collections of clinical isolates. Nine human-adapted lineages of the Mtb complex have been classified to date, including Mtb *sensu stricto* (lineages 1–4 and 7) and *M. africanum* (lineages 5 and 6) [5]. Lineages 8 and 9 were more recently identified [6,7]. A higher level of genetic and molecular diversity than anticipated has been found between lineages, including differences in the transcriptome, proteome and metabolome

* Corresponding author. London School of Hygiene and Tropical Medicine, Keppel Street, London, WC1E 7HT, UK.
E-mail address: hannah.painter2@lshtm.ac.uk (H. Painter).
[1] Department of Life Sciences, College of Health, Medicine and Life Sciences, Brunel University London, Kingston Lane, UB8 3PH, UK.

https://doi.org/10.1016/j.tube.2024.102494
Received 6 December 2023; Received in revised form 5 February 2024; Accepted 11 February 2024
Available online 13 February 2024

[8–14]. The host response to infection has also been shown to vary in humans and animal models, with differences in growth rate, virulence, presentation of disease, and induction of innate and adaptive immunity reported [15–22].

In the context of preclinical vaccine evaluation, most experimental infection is performed using laboratory strains such as Mtb Erdman, CDC1551 and H37Rv. These strains have been passaged for decades in the laboratory resulting in adaptation to laboratory conditions, and are all classified as lineage 4 [4,23]. It has been proposed that historical reliance on laboratory strains may explain, in part, why observations in animal models can translate poorly into human studies. While limited, studies which have evaluated vaccine-induced protection against non-laboratory strains have shown variation in protection compared with laboratory strains, indicating that incorporation of representative clinical isolates into routine preclinical vaccine testing may improve future translation into clinical studies [2,24–29].

The direct mycobacterial growth inhibition assay (MGIA) represents a cost-effective and 3Rs-compliant [23] tool which could permit the high-throughput evaluation of candidate TB vaccine efficacy against multiple strains of Mtb in parallel. The MGIA is a functional assay proposed to replicate a range of host immune mechanisms and complex interactions *ex vivo* [30]. The summative capacity of a mixed population of primary host cells and other immune factors to control mycobacterial growth is determined by *ex vivo* co-culture with mycobacteria for a defined period, followed by quantification of mycobacterial load. Where host phenotype and/or intervention confers an enhanced ability to regulate mycobacterial growth, growth inhibition is observed compared with a selected control. A range of human and animal assays have been described in the literature [31–37], including for mouse lung [34] and spleen [37]. In the murine spleen direct MGIA, as well as human and non-human primate peripheral blood mononuclear cell (PBMC) direct MGIAs, vaccine-mediated mycobacterial growth inhibition correlates with protection *in vivo* [35–40]. A comparison of the murine lung direct MGIA with *in vivo* protection has not yet been reported [34].

The suitability of the murine direct MGIA for more comprehensive vaccine evaluation is supported by the minimal input requirements for the assay. Following experimental challenge with Mtb *in vivo*, one animal provides one data point per organ. By contrast, in the MGIA each organ harvested provides the opportunity for multiple assessments under different co-culture conditions, facilitating screening against different Mtb strains. Vaccine evaluation may be expanded further using cells from the same animals for other immunological analysis methods to gain biological insight into mechanisms driving protection. Table 1 provides a summary of the parameters of an *ex vivo* MGIA and *in vivo* experimental infection with Mtb, highlighting how the MGIA comparatively reduces study length, number of mice, and facilities required to test novel TB vaccines.

Table 1
Comparison of parameters of the *ex vivo* MGIA versus *in vivo* Mtb experimental infection for a three-group study design using four mycobacterial strains.

Parameter	MGIA	Mtb experimental infection
Mice, n/group	Minimum 3	8–10 per Mtb strain[a]
Total mice for proposed study design, n	9	96 + 12[b]
In vivo experiment duration, weeks	6[c]	11[c]
Ex vivo experiment duration, days	4–6	–
Time to results post-takedown, weeks	2	3
BSL-3 animal facility required?	No	Yes
BSL-3 microbiology facility required?	Yes	Yes

Information in rows 1–3 is specific to the study design: three group design (i.e. BCG + novel candidate vaccine + unvaccinated) with four mycobacterial strains and should be adjusted accordingly.

[a] The Lamorte power calculation tool was used to approximate sample size to detect a 1 log reduction in CFU.

[b] 3 mice per strain for confirmation of infection.

[c] MGIA takedown/Mtb infection timepoint defined by vaccine-specific immune response peak; duration of infection should be adjusted for factors such as infection dose, mouse strain and mycobacterial strain virulence, and be based on defined humane end points.

To the best of our knowledge, non-laboratory strains have not previously been used as the inoculum in the direct MGIA, and no studies to date have screened responses to a panel of mycobacteria in parallel. Considering the growing interest in the Mtb complex and relevance of variation in vaccine efficacy against different strains, the murine lung and spleen MGIAs represent a potential tool to expand on the readout feasibly obtained from experimental *in vivo* studies.

We provide proof-of-concept demonstrating how the murine MGIA may be used to evaluate vaccine-mediated growth inhibition of clinical isolates from different lineages of the Mtb complex. The biological relevance of the assay as a surrogate of protective efficacy was assessed by performing a head-to-head comparison of the MGIA and an *in vivo* experimental Mtb infection study. Further, we expanded on the application of the MGIA by incorporating flow cytometry and RNA-seq analysis into the workflow. The host cell lung preparations utilised in the MGIA were analysed by these methods to identify potential correlates of growth inhibition, and determine the extent to which these vary by Mtb strain.

2. Materials and methods

2.1. Ethics statement

Animal experimentation was performed under licence PPL 70/8043 (superseded by P6CA9EB8D) issued by the UK Home Office according to the Animals (Scientific Procedures) Act 1986 and approved by the London School of Hygiene & Tropical Medicine (LSHTM) Animal Welfare and Ethics Review Body. This manuscript was prepared in accordance with the ARRIVE guidelines [41].

2.2. Mycobacterial strains

BCG Pasteur Aeras was obtained from Aeras (USA). The reference set of Mtb complex clinical strains was kindly donated by Professor Sebastian Gagneux (Swiss Tropical and Public Health Institute, Switzerland) [4]. Mtb clinical isolates from lineage 1 (L1 N0072), lineage 2, (L2 N0052) and lineage 4 (L4 N1283) were used in the study. All mycobacteria were grown to mid-log phase in Middlebrook 7H9 (Yorlab, UK) broth supplemented with 10% OADC (Yorlab), 0.05% Tween 80 and 0.2% glycerol and stored in aliquots at −70 °C. The CFU of all frozen stocks was determined by serial dilution on 7H11 (Yorlab, UK) agar plates (10% OADC, 0.5% glycerol). All work using Mtb was performed in aerosol-containment biosafety level-3 (BSL-3) laboratories at LSHTM in accordance with guidance from the UK Advisory Committee on Dangerous Pathogens.

2.3. Animals

Female C57BL/6 mice (5–7 weeks old; weight 16–20 g) were obtained from Charles River UK and rested for at least five days before commencing procedures. Animals were housed in individually ventilated cages (maximum six animals/cage) in the LSHTM Biological Services Facility (BSF) with access to food and water *ad libitum*. Mice infected with Mtb were housed in isolators under BSL-3 containment. Animals were randomly assigned to cages on arrival by staff in the BSF. Each cage was randomly assigned a group number on commencement of the study.

2.4. Immunisation

BCG Pasteur Aeras was thawed at room temperature and diluted in saline solution (Baxter Healthcare, UK) to a final concentration of 10^7 CFU/ml. BCG was administered as 100 μl (1×10^6 CFU) subcutaneously

into the right or left leg flap using a sterile 27G needle. Control animals received no treatment. Animals were rested for six weeks following vaccination before i) harvesting organs to generate single cell suspensions for the *ex vivo* MGIA or ii) *in vivo* infection with Mtb was performed.

2.5. In vivo Mtb infection

Mice were infected via the intranasal route with L1 (N0072) or L2 (N0052). Frozen aliquots of mycobacteria were thawed at room temperature and diluted in saline to a concentration of 7.5 x 10^3 CFU/ml. Mice were anaesthetised by intraperitoneal injection of a combination of ketamine (65 mg/kg; Ketalar, Pfizer Ltd, UK) and xylazine (10 mg/kg; Rompun, Bayer plc, UK) in saline, followed by delivery of 40 μl inoculum equally between the two nostrils. Confirmation of the infection dose was performed one day after infection by determination of the number of viable mycobacteria in the lungs of three mice (L1: 280–360 CFU; L2: 220–340 CFU). Remaining mice were housed for five weeks following Mtb infection with daily health monitoring and weekly weight checks. The study was terminated by cervical dislocation, and lungs and spleens were collected and homogenised in PBS-tween 80 (0.05%). Total bacterial load per organ was quantified by plating appropriate serial dilutions of homogenate on 7H11 agar plates and incubating plates at 37 °C for three weeks.

2.6. Lung and spleen cell isolation for ex vivo analyses

Lung and spleen cell populations were generated from excised organs as described previously [34] and used downstream in the *ex vivo* MGIA. Lung cells were also analysed by RNA-seq or flow cytometry. For the MGIA, technical replicates for the co-culture were generated using a single pool of cells per group isolated from six mice. Cells from individual mice were used as biological replicates for RNA extraction and flow cytometry.

2.7. Ex vivo mycobacterial growth inhibition assay (MGIA)

The *ex vivo* MGIA was performed as described previously [34]. Briefly, lung ($1x10^6$) or spleen ($3x10^6$) cells were co-cultured with mycobacteria in 48-well plates (BioLite; Fisher Scientific, UK). Plates were incubated at 37 °C (5% CO2) for 4–6 days. Following incubation, supernatants were removed, and adherent host cells were lysed with 500 μl sterile water. Mycobacterial CFU was quantified in the lysate by adding the total lysate to PANTA-supplemented mycobacterial growth indicator tubes (MGITs) (BD, UK). MGITs were placed in the BACTEC MGIT 320 system (BD) until registered positive with time to positivity (TTP) values. To convert TTP to mycobacterial CFU, standard curves were produced for each Mtb isolate as described previously [42].

2.8. Flow cytometry

Following cell isolation from the lung, $1x10^6$ cells per sample were stained with live/dead fixable blue dead cell stain kit (Thermo Fisher, UK) according to the manufacturer's instructions. Cells were washed with PBS and fixed with 1X Phosflow lyze/fix buffer (BD) at 37 °C for 30 min. Following fixation, samples were washed with FACS buffer (PBS + 2% FBS), incubated with Fc block (anti-mouse CD16/CD32; eBioscience, UK) for 10 min and then stained for 30 min at 4 °C, protected from light, with a mixture of fluorochrome-conjugated antibodies (detailed in Table 1) prepared in Brilliant Stain buffer (BD). Following staining, cells were washed and resuspended in FACS buffer. Antibody and live/dead stain compensation was performed using OneComp eBeads Compensation Beads (Thermo Fisher) or the ArC Amine Reactive Compensation Bead kit (Thermo Fisher) respectively. Data were acquired on an LSRII flow cytometer using FACSDiva software (BD), and analysed using FlowJo (v10.4, FlowJo LCC, USA). The gating strategy is shown in Fig. S1 and was developed using a combination of two published gating strategies for murine lung [43,44]. Total counts for individual populations were calculated using the following formula: total number of target cell population per lung = total count cells per lung x (count population of interest/count live cells). Total count cells per lung was determined by trypan blue exclusion method; count live cells was determined by gating on cells negative for live/dead fixable blue dead stain.

2.9. Ex vivo cell culture and RNA extraction

Lung cells from individual mice were used for RNA extraction. Specifically, $1x10^6$ cells per mouse were seeded in duplicate (uninfected/infected) in 24-well plates (BioLite, Fisher Scientific) and cultured overnight at 37 °C (5% CO2) in the presence or absence of 1×10^6 CFU mycobacteria (N0072, N0052 or N1283). An MOI of 1 was selected for gene expression analysis based on experimental conditions described previously by Marsay et al. [38]. Mycobacterial input was confirmed by plating on 7H11 agar plates. The following day, the 48-well plates were centrifuged at 500×*g* to pellet eukaryotic cells, supernatants were removed and 600 μl RNAprotect cell reagent (Qiagen, UK) was added to stabilise transcription and prevent RNA degradation. Samples were stored at −70 °C until RNA extraction. For RNA extraction, samples were thawed and centrifuged at 5000×*g*. Total RNA purification was performed using the RNeasy Mini Kit and an on-column DNase digestion according to the manufacturer's instructions (both Qiagen). RNA integrity was assessed, and concentration determined, using the TapeStation system (Agilent, UK). All samples submitted for sequencing had an RNA integrity number equivalent value ≥ 8.2.

2.10. Library preparation and sequencing

Library preparation and sequencing was performed at UCL Genomics (University College London, UK). The NEBNext Ultra II Unidirectional RNA library prep kit and Poly(A) mRNA Magnetic Isolation Module (both New England Biolabs, UK) were used to process 200 ng total RNA per sample according to the manufacturer's instructions. Limited cycle PCR was performed with 100 ng for 14 cycles. Libraries to be multiplexed in the same run were pooled in equimolar quantities, calculated from Qubit (Invitrogen, UK) and Bioanalyzer (Agilent) fragment analysis. Samples were sequenced on the NextSeq 500 (Illumina, UK) instrument using a 75-bp single read run with a corresponding 8-bp UMI read.

2.11. RNA-seq data analysis

Sample processing from fastq files to the generation of a read count matrix was performed on the Linex-based high performance computing service at LSHTM. The BBDuk tool from the BBTools suite [45] (v38.79) was used to trim adaptor sequences and the final 5% of 3' bases. *Mus musculus* genome FASTA (ftp://ftp.ensembl.org/pub/release-99/fasta/mus_musculus/dna/Mus_musculus.GRCm38.dna.primary_assembly.fa.gz) and gene annotation GTF (ftp://ftp.ensembl.org/pub/release-99/gtf/mus_musculus/Mus_musculus.GRCm38.99.gtf.gz) files were downloaded from Ensembl [46]. STAR [47] (v2.7.3a) was used to generate a genome index and subsequently map the trimmed reads to the *Mus musculus* index. Read counting was performed using the default settings of featureCounts [48] to count meta-features, specifying a stranded dataset. Quality control steps were performed using FastQC (v0.11.9) [49] and CollectRnaSeqMetrics from the Picard Tools suite [50]. Differential gene expression analysis was performed using the R/Bioconductor package DESeq2 [51] (v1.28.1) in the R environment (v3.6.1). Hypothesis testing in the DESeq function was performed using the Wald test. Results tables for comparisons were built using contrast to obtain $\log_2$ fold change (LFC) values and associated statistics for multiple condition effects. Multiple correction was performed using the

Benjamini–Hochberg method [52].

2.12. Mouse lung module enrichment analysis

A set of 38 murine lung modules generated previously by Singhania et al. [53] were used to perform module enrichment analysis. Modules were pre-processed for use in the tmod package [54]. The makeTmod function was used to generate a tmod object. For LFC data for each condition of interest, a metric score for each differentially expressed gene (>/< 0) was calculated using the equation:

$$\text{metric} = -\log_{10}(\text{adjusted p}) \times \text{abs}(\text{LFC})$$

Results were set in descending order to generate ranked Ensembl ID lists. Transcriptional module analysis of the lists was performed using the CERNO test [55] and visualised using the tmodPanelPlot. tmodPanelPlot generates a heatmap-like representation which includes the effect size (area under the receiver operating curve [AUROC]) and adjusted p (padj) values for modules enriched in the conditions of interest. All 38 modules from the Singhania set are shown with an enrichment threshold of padj <0.01 used. Since ordered lists for module enrichment analysis are not generated using a p-value threshold, the proportion of individual genes within each module identified to be significantly up- or downregulated were visualised as a 'pie' using the tmodDecideTests function of the tmod package for each result: red, upregulated (padj <0.05); blue, downregulated (padj <0.05); grey, not significant.

2.13. Statistical analysis

All statistical analyses were carried out using GraphPad Prism Software version 9.4.1 (GraphPad, USA). Statistical significance was tested using the unpaired *t*-test with Welch's correction; a p value of <0.05 was considered statistically significant and is denoted with asterisk in the figures where appropriate.

3. Results

3.1. Evaluation of BCG vaccine-mediated growth inhibition of different Mtb clinical isolates using the direct lung and spleen MGIA

Vaccine-mediated growth inhibition of the laboratory strain, Mtb Erdman, by murine cells has been previously demonstrated by MGIA [34,40]. To determine whether the MGIA could be expanded to explore potential differences in vaccine-mediated growth inhibition beyond this single strain, clinical isolates from a well-characterised clinical reference set were used in the direct lung and spleen assay [4].

Since variations in the growth rate of different lineages of the Mtb complex have been reported *in vitro* and *ex vivo* [17,20,56–60], we hypothesised that the dynamics of vaccine-mediated growth inhibition in the MGIA may vary by clinical isolate. A lineage 1 (L1 N0072) isolate, classified as an East-African-Indian ancient lineage of the MTB complex, and a lineage 2 isolate (L2 N0052), classified as a modern lineage of the Beijing sub-lineage, were selected for optimisation of the assay [34,37]. *Ex vivo* co-culture of lung and spleen cells from BCG-vaccinated and unvaccinated mice with the clinical isolates was performed for 4, 5 or 6 days before the cells were lysed, and mycobacterial load was quantified. Mycobacterial load across the time course is shown in Fig. S2. Significant growth inhibition of lineage 2 was observed using lung and spleen cells from BCG-vaccinated mice compared with control mice following four-, five- and six-day co-cultures. Vaccine-mediated growth inhibition of the lineage 1 clinical isolate was also observed for all co-culture periods with lung cells but was not detectable in the spleen co-cultures until day 6. At this time point, vaccine-mediated growth inhibition in the other co-cultures remained at a comparable level to earlier time points; therefore, this timepoint was utilised for further MGIA studies for the clinical isolate panel.

Following optimisation, a lineage 4 isolate, a modern Euro-American lineage was also analysed by the MGIA. Specifically, lung cells and splenocytes were inoculated with Mtb lineages 1, 2 and 4 for a six-day co-culture period. Compared with unvaccinated control mice, a significant reduction in mycobacterial growth was observed for BCG-vaccinated mice across the three mycobacterial strains for both lung (L1 N0072, 0.45 $\log_{10}$ CFU, $p < 0.0001$; L2 N0052, 0.39 $\log_{10}$ CFU, $p = 0.0025$; L4 N1283, 0.41 $\log_{10}$ CFU, $p = 0.0005$) and spleen (L1 N0072, 0.22 $\log_{10}$ CFU, $p = 0.0028$; L2 N0052, 0.21 $\log_{10}$ CFU, $p < 0.0001$; L4 N1283, 0.70 $\log_{10}$ CFU, $p = 0.0028$) assays (Fig. 1).

3.2. Validation of the direct lung and spleen MGIA against in vivo challenge with different Mtb clinical isolates

To determine whether mycobacterial control observed in the lung and spleen MGIA reflects bacterial burden following *in vivo* infection with Mtb clinical isolates, an Mtb experimental infection study was performed. Due to feasibility, one ancient and one modern lineage clinical isolate were selected for experimental infection: L1 N0071 and L2 N0072. Six weeks following BCG vaccination, mice were intranasally infected with approximately 300 CFU per Mtb isolate. At five-weeks post infection, a significant reduction in L1 and L2 bacterial burden was observed in the lung and spleen of BCG-vaccinated animals compared with unvaccinated animals (L1 lung, 1.09 $\log_{10}$ CFU, $p < 0.0001$; L1 spleen, 0.80 $\log_{10}$ CFU, $p = 0.0004$; L2 lung, 0.88 $\log_{10}$ CFU, $p = 0.0001$; L2 spleen, 0.75 $\log_{10}$ CFU, $p < 0.0001$) (Fig. 2). There was no difference in magnitude of BCG vaccine-mediated control of the two isolates. These observations are consistent with the *ex vivo* MGIA in which enhanced mycobacterial control of both L1 and L2 was observed by BCG-vaccinated lung and spleen cells following six-day co-culture compared with cells from unvaccinated mice (Fig. 1).

3.3. The cell composition of murine lung samples is altered following intradermal BCG vaccination and is associated with enhanced control of mycobacterial growth

It has previously been shown *in vivo* that intradermal BCG vaccination is able to induce a persistent, long-lived population of polyfunctional $CD4^+$ T cells in the lungs which preferentially expand following Mtb challenge and associate with BCG-induced protection [61]. We thus explored whether the composition of the murine lung cell preparation used in the MGIA is influenced by BCG vaccination and similarly influences *ex vivo* outcomes. Fig. 3a depicts the relative frequencies of ten major immune cell populations as a percentage of the total live cell population. The relative frequency of CD45-negative cells (non-haematopoietic, lung parenchymal cells) is also shown. The mean group frequency of each population is visualised in Fig. 3b. In the lung cell preparation from BCG-vaccinated mice, which demonstrated enhanced control of mycobacterial growth against all isolates tested, we observed a significant increase in the proportion of $CD103^+$ DCs (0.69 vs 1.0%, $p = 0.0138$), $CD11b^+$ DCs (2.5 vs 7.9%, $p = 0.0055$) and interstitial macrophages (1.0 vs 2.1%, $p = 0.0095$), and decrease in B cells (25.7 vs 20.3%, $p = 0.0310$) and eosinophils (2.2 vs 1.5%, $p = 0.0491$), when compared with control mice. The total number of $CD103^+$ and $CD11b^+$ DCs was also significantly increased in the vaccinated lung (Fig. S3).

Further, the transcriptional profile of lung cell preparations from control and BCG-vaccinated mice was analysed by RNA-seq. Differential gene expression analysis between BCG-vaccinated lung versus control lung was performed and used to generate ordered gene lists for enrichment analysis using a set of murine lung modules [53]. Enrichment was determined using the coincident extreme ranks in numerical observations (CERNO) test and is visualised in Fig. 4. Enrichment of modules dominated by macrophage-, granulocyte-, and myeloid-specific genes were found (modules 3, 10–14). In modules 10 and 11, individual genes visualised as significantly perturbed were largely downregulated.

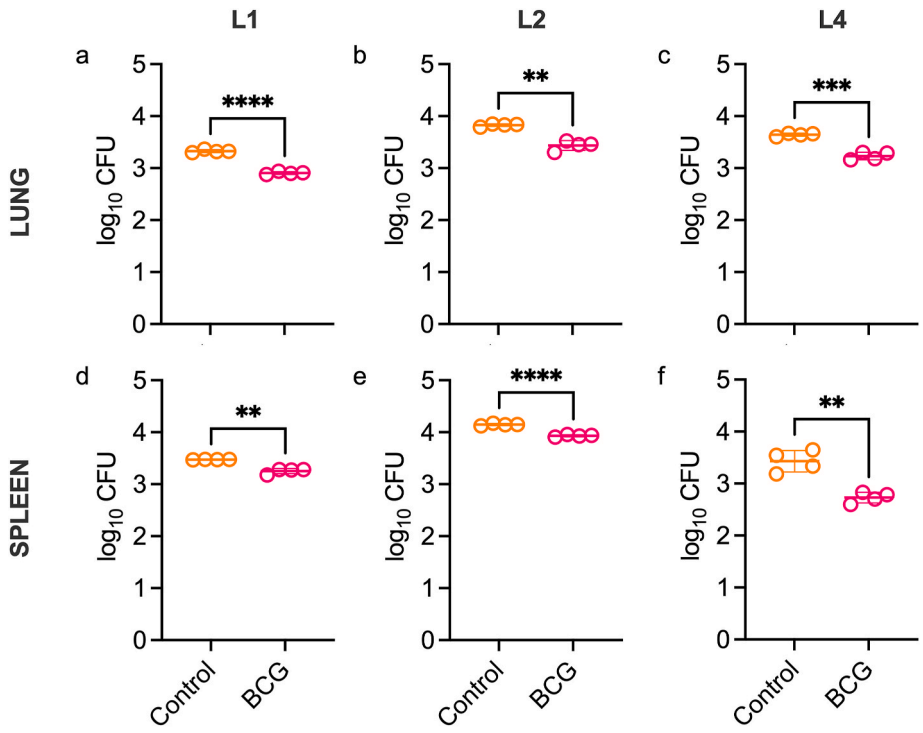

Fig. 1. Growth inhibition of Mtb clinical isolates by BCG-vaccinated versus unvaccinated murine cells. C57BL/6 mice (n = 6/group) received BCG or no treatment (control). Six weeks post-vaccination, lung and spleen cells were co-cultured with 200 CFU [a and d] L1 (N0072), [b and e] L2 (N0052) or [c and f] L4 (N1283). At six days post co-culture, samples were lysed and transferred to the BACTEC system until TTP values were generated. TTP values were converted to $\log_{10}$ CFU based on a standard curve. Data points (n = 4/group) represent samples generated from pooled cells isolated from six mice. Statistical significance was tested by unpaired *t*-test with Welch's correction. Error bars represent mean ± standard deviation. **p < 0.01; ***p < 0.001; ****p < 0.0001.

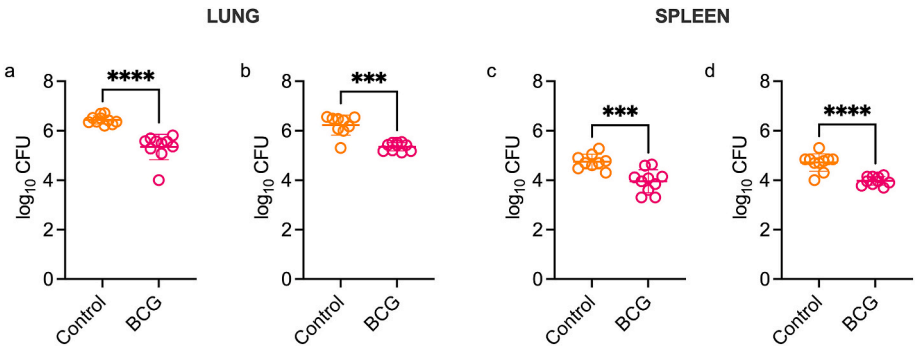

Fig. 2. BCG vaccination reduces mycobacterial burden in the lung and spleen of mice challenged with L1 (N0072) or L2 (N0052). C57BL/6 mice (n = 9–10 mice/group) received BCG or no treatment (control). Six weeks following vaccination, mice were intranasally infected with ~300 CFU [a and c] L1 (N0072) or [b and d] L2 (N0052). CFU per organ was determined five-weeks post-infection in the lung and spleen (n = 9–10/group). Statistical significance was tested by unpaired *t*-test with Welch's correction. Error bars represent mean ± standard deviation. ***p < 0.001; ****p < 0.0001.

By contrast in modules 3, 13 and 14, significant genes were upregulated. Enrichment of modules 5 (Type I IFN/Ifit/Oas), 6 (Cell cycle/Stem cells/Chemokine receptors), 7 (Ifng/Stat1/Gbp/Antigen presentation), 8 (Glycolysis), 35 (Cytotoxic/T cells/NK/Tbx21/Eomes/B cells), 36 (NK cells/Leukocytes/Cytotoxic) and 37 (B & T cells/Myeloid cells) was also identified. Enrichment of modules 3, 5, 6, 7, 13, 14, 35 and 37 was validated in an independent experiment of the same design (Fig. S4).

3.4. Ex vivo infection of murine lung cells induces Mtb isolate-specific transcriptional changes that are not associated with differential control of mycobacterial growth

To identify potential transcriptional correlates of mycobacterial growth control, RNA was extracted from lung cells co-cultured with the L1, L2 or L4 clinical isolates. Enrichment of the murine lung modules in lung cells from BCG vaccinated compared with unvaccinated mice is visualised for the three isolates in Fig. 5. Consistently across the three isolates, *ex vivo* infection of lung cells from BCG-vaccinated mice was associated with higher levels of enrichment of many of the modules identified in uninfected lung cells from BCG-vaccinated mice (Fig. 4; modules 1, 3, 7, 12–14 and 35). Modules 21 (a module annotated as miscellaneous, and reported as enriched in macrophages and granulocytes [53]) and 33 (Diverse intracellular signalling) were also enriched across the three isolates.

Despite the finding that BCG-vaccinated lung cells exhibit similar capacity to inhibit growth of the three Mtb isolates, several lung modules were found to be uniquely enriched following *ex vivo* infection with specific lineages. Infection with L1 was associated with perturbation of genes enriched for Type I IFN/Ifit/Oas (module 5) and two modules associated with cell signalling (modules 17 and 32). Enrichment of an

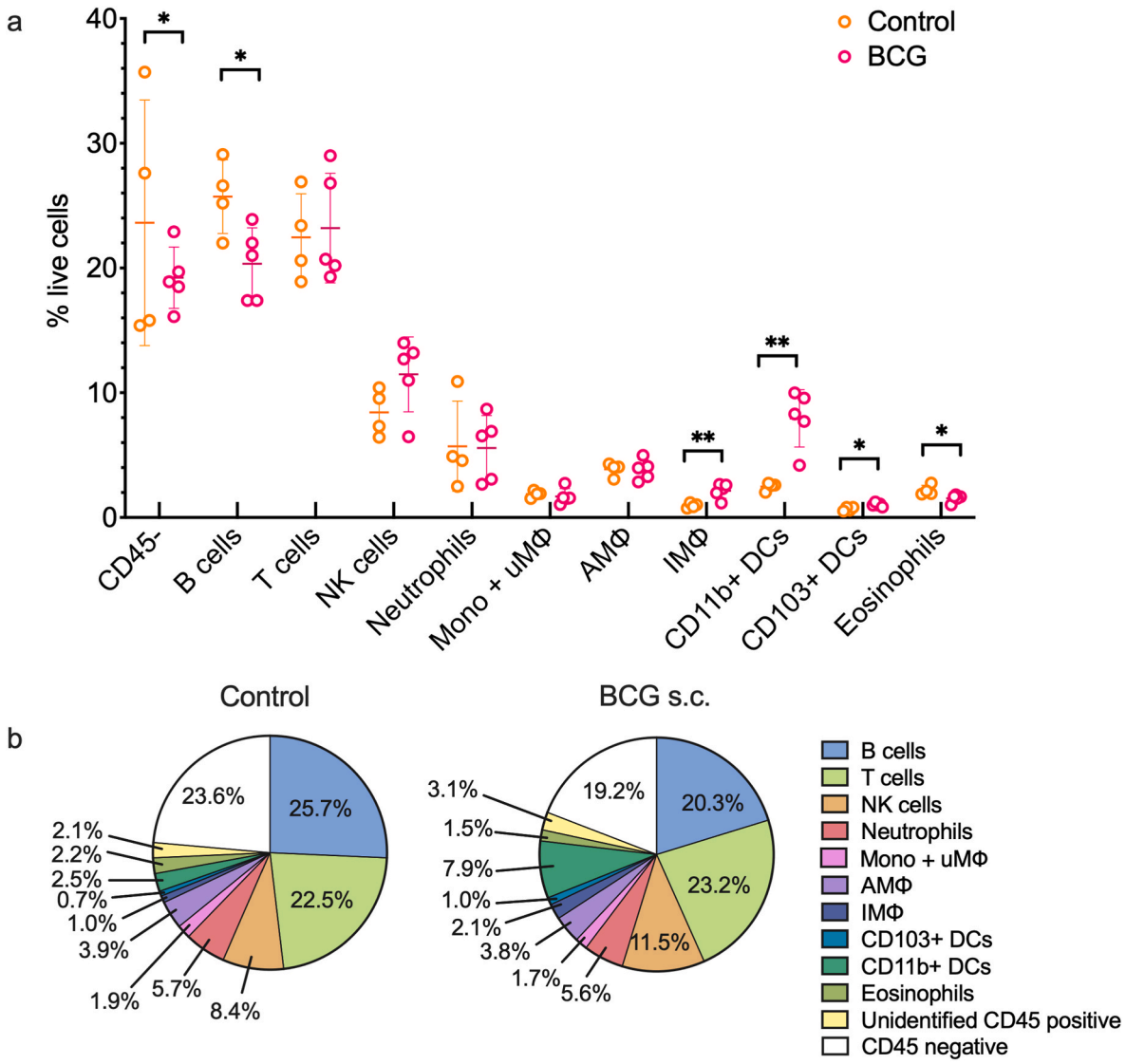

Fig. 3. Cell populations in the murine lung MGIA input. C57BL/6 mice (n = 5/group) received BCG or no treatment (control). Six weeks post-vaccination, lungs were processed to generate a single cell suspension which was stained with an antibody cocktail. [a] Identified cell populations in the lung as a percentage of live cells are shown. Statistical significance was tested using the unpaired *t*-test with Welch's correction. Error bars represent mean ± standard deviation. *p < 0.05; **p < 0.01. [b] Pie charts depict the relative frequencies of identified immune cell types in the lung as a percentage of live cells in control and BCG-vaccinated lung (mean of 4–5 individual mice). AMΦ, alveolar macrophages; DC, dendritic cell; IMΦ, interstitial macrophages; NK, natural killer; uMΦ, undifferentiated macrophages.

intracellular signalling module (module 28) was found with L2 only. Modules related to inflammation and metabolism (module 2) and glycolysis (module 8) were unique to infection with L4. Together, L2 and L4 were associated with enrichment of genes related to Cell cycle/Stem cells/Chemokine receptors (module 6), myeloid/granulocyte function modules 10 and 11 and NK cells/Leukocytes/Cytotoxic (module 36).

4. Discussion

Despite growing recognition of the importance of testing TB vaccines against clinical isolates prior to progression into the clinical pipeline, use of non-laboratory strains in the murine MGIA has been limited [62,63]. In the current study, lung and spleen cells from BCG-vaccinated mice were shown to significantly inhibit growth of three Mtb clinical isolates when compared with cells from unvaccinated mice using the direct MGIA. By running an experimental infection study alongside the *ex vivo* MGIA, we demonstrate that *ex vivo* BCG-mediated growth inhibition is consistent with BCG-mediated protection in the lung and spleen *in vivo*, indicating that this methodology may offer a biologically relevant approach to predict vaccine-induced protection against multiple Mtb lineages prior to testing in *in vivo* infection studies.

The immunological mechanisms driving growth inhibition in the direct murine lung MGIA have not been characterised. In the direct splenocyte MGIA, Marsay et al. performed microarray analysis in parallel with the assay. Following *ex vivo* infection with BCG, an enhanced T_H1 response, including increased expression of interferon (IFN)-γ, nitric oxide synthase and interleukin (IL)-17, was reported to correlate with *ex vivo* BCG-mediated growth inhibition [38]. With the aim of identifying 'correlates of growth inhibition' in the lung MGIA, we incorporated flow cytometry and RNA-seq into the MGIA workflow to analyse the host cellular response following *ex vivo* infection with multiple clinical strains of mycobacteria, as well as to characterise the host cell populations within the MGIA co-culture. Compared with lung cell populations generated from unvaccinated mice, we found differences in the cellular composition and transcriptome of lung from BCG-vaccinated mice, reflective of differences in both adaptive and innate immunity.

Focusing first on the composition of the host cells within the lung MGIA, the lung cell population generated from BCG-vaccinated mice at

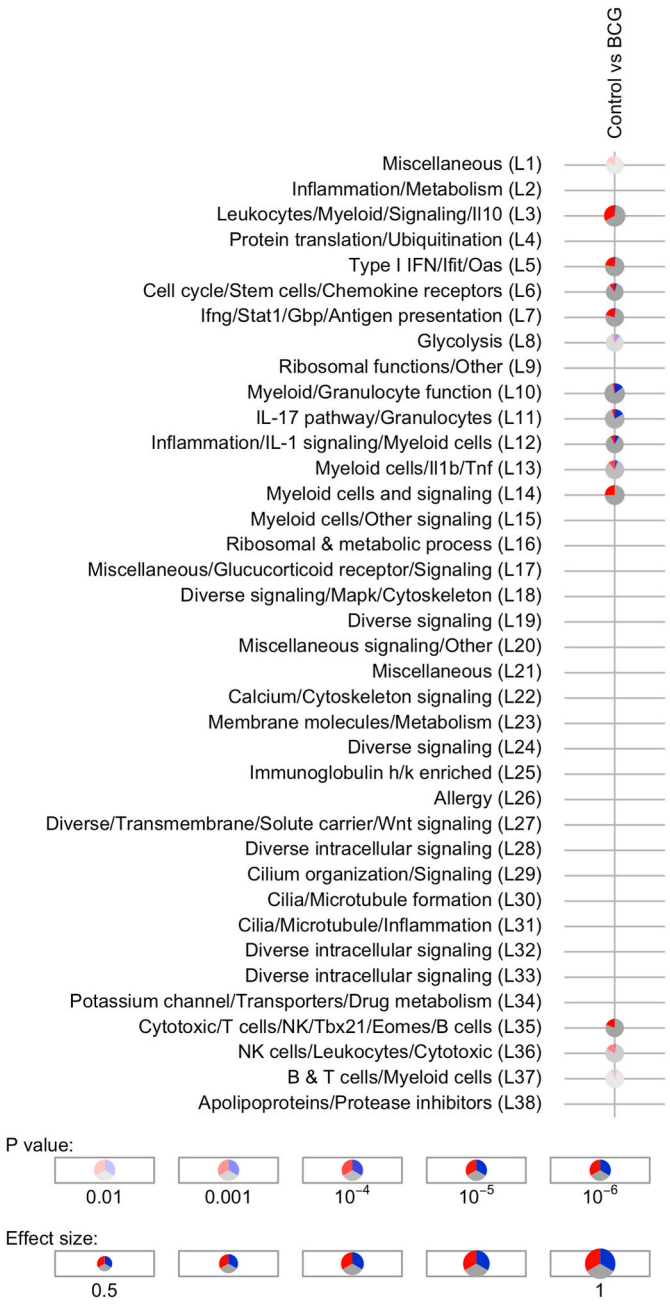

Fig. 4. tmod analysis of processed host MGIA input. C57BL/6 mice (n = 3/group) received BCG or no treatment (control). Six weeks post-vaccination, single cell suspensions were generated from lungs, and RNA was extracted and analysed by RNA-seq. tmodPanelPlot visualising enrichment in defined murine lung modules for differentially expressed genes in BCG-vaccinated lung versus control. Each row contains one module. Modules found to be significantly enriched (padj <0.01) are indicated by a grey circle (pie), with the degree of significance indicated by colour intensity and the effect size (AUROC) indicated by size. The proportion of individual genes within each module found to be significantly (padj <0.05) up- or downregulated are marked in each pie in red or blue respectively. (For interpretation of the references to colour in this figure legend, the reader is referred to the Web version of this article.)

six weeks post-vaccination contained an increased proportion of $CD103^+$ DCs, $CD11b^+$ DCs and interstitial macrophages, and a decrease in B cells and eosinophils, compared with lung populations from naïve mice. Further, the transcriptome of these cells was enriched for gene modules annotated to type-I IFN, natural killer (NK) cells and cytotoxicity, IFNγ and macrophage-, granulocyte-, and myeloid-specific genes.

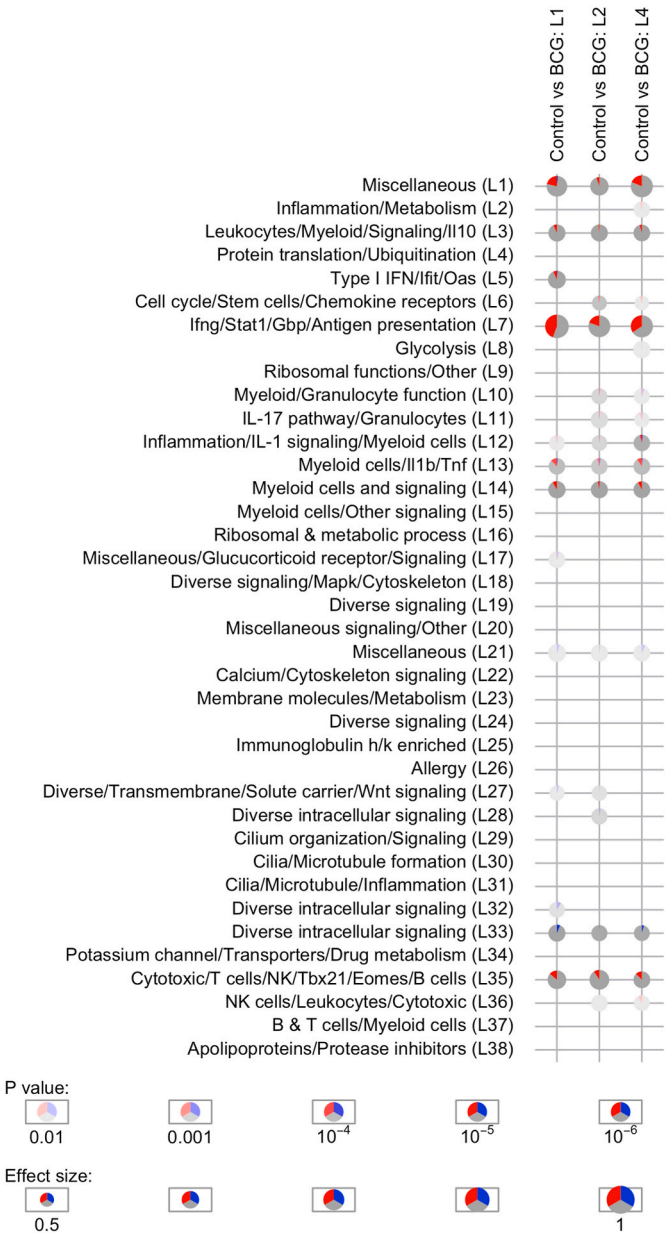

Fig. 5. Modular transcriptional enrichment correlates with BCG-mediated growth inhibition in the MGIA. C57BL/6 mice (n = 3/group) received BCG or no treatment (control). Six weeks post-vaccination, single cell suspensions were generated from lungs and co-cultured overnight with L1 (N0072), L2 (N0052) or L4 (N1283). RNA was extracted and analysed by RNA-seq. tmodPanelPlot visualising enrichment in defined murine lung modules for differentially expressed genes in BCG-vaccinated lung cells versus control. Modules found to be significantly enriched (padj <0.01) are indicated by a grey circle (pie), with the degree of significance indicated by colour intensity and the effect size (AUROC) indicated by size. The proportion of individual genes within each module found to be significantly (padj <0.05) up- or downregulated are marked in each pie in red or blue respectively. (For interpretation of the references to colour in this figure legend, the reader is referred to the Web version of this article.)

Following subcutaneous vaccination, live BCG bacilli disseminate to numerous sites and have been detected in the lung at six weeks post vaccination and beyond [64] and the level of BCG distribution in the lungs of mice has been associated with protection from Mtb challenge [65]. It is, therefore, likely that our observed differences in lung immune cell populations and corresponding enhanced *ex vivo* Mtb growth inhibition in cells from BCG-vaccinated mice is reflective of a recently

cleared or existing low level of BCG present in the lung following vaccination.

Several immune cell types found to be enriched in the BCG-vaccinated lung have been previously reported to play a protective role against Mtb infection. For example, interstitial macrophages have been shown to host Mtb in a nutritionally restrictive environment which tempers mycobacterial growth. This is in direct comparison to alveolar macrophages which provide a more metabolically advantageous environment to Mtb which facilitates growth [66]. In addition, depletion of NK cells following BCG vaccination has been shown to inhibit BCG-induced protection against experimental infection with Mtb in the mouse model [67]. The enhanced NK cell transcriptional signal identified in our MGIA input from vaccinated mouse lung may be driven, at least in part, by IL-12 production from the enhanced proportion of DCs also observed. Few studies have evaluated the immune status of the BCG-vaccinated murine lung prior to Mtb challenge. Aranday–Cortes et al. identified a pulmonary gene expression signature related to connective tissue development six weeks following vaccination [68]. Irwin et al. reported activation of a pulmonary adaptive T-cell response up to six weeks following BCG vaccination in mice which correlated with protection following H37Rv infection *in vivo* [69].

In addition to induction of type II IFN signalling, we found that BCG vaccination induced a type I IFN signal in the lung. The role of type-I IFNs in Mtb infection is complex, and timing of the signal with respect to infection appears to define whether a pathogenic or protective effect is observed. High levels of type I IFNs during infection with hypervirulent Mtb strains are associated with pathogenesis in humans and mice [70–74]. However, type-I IFNs have been shown to contribute to early control of BCG, *M. avium* and *M. smegmatis* infection in the murine lung [75–77]. Further, early tonic type I IFN signalling has been demonstrated to prime innate immune cells for production of proinflammatory cytokines protective against TB [73]. Consistent with our own findings, Mai et al. [78] reported that the profile of the airway landscape in C57BL/6 mice receiving subcutaneous vaccination with BCG was altered compared with unvaccinated controls. In addition to shifts in T cells and DCs, subpopulations of alveolar macrophages were identified in the vaccinated airway, defined by expression of interferon-stimulated genes, oxidative stress response and interstitial macrophage-like profiles.

Following *ex vivo* infection with clinical Mtb isolates, many of the modules enriched in vaccinated lung cells used as input in the MGIA remained enriched across the three lineages, consistent with our observation that BCG-vaccinated lung cells inhibit growth of three clinical isolates to a similar capacity with regards to mycobacterial load. However, several modules were found to be enriched in specific lineages only. These differences may reflect variations in the mechanisms by which BCG vaccine-mediated immunity controls the growth of different Mtb isolates, but may not ultimately translate into a net difference in overall capacity to control mycobacterial growth. This is supported by the finding that the magnitude of BCG-induced protection did not differ following *in vivo* challenge with two of the clinical isolates.

Gene enrichment of the type-I IFN signalling module as a correlate of growth inhibition by BCG-vaccinated lung cells remained following *ex vivo* infection with the lineage 1 isolate only. The highly virulent Mtb strains, W4 and HN878 (both lineage 2 Beijing strains), have been shown to induce higher levels of type-I IFN signalling than CDC1551. These higher levels of type-I IFN led to reduced T_H1 immunity and reduced survival of Mtb-infected mice [71]. This may indicate that the type-I IFN signal in the murine lung induced by BCG vaccination in the current study may be overwhelmed by induction of type-I IFN signalling following *ex vivo* infection with the lineage 2 and 4 isolates, no longer contributing to mycobacterial control. Enrichment of genes associated with the IL-17 pathway/Granulocytes (module 11) and Inflammation/IL-1 signalling/Myeloid cells (module 12) was identified in cells from BCG-vaccinated mice following *ex vivo* infection with the lineage 2 and 4 isolates. In the mouse model, Gopal et al. report that early protective immunity against HN878 is driven by high IL-17 levels induced by production of IL-1β via a TLR2-dependent mechanism. However, IL-17 was found to be disposable for protection against the laboratory strains, H37Rv and CDC1550 [79].

The BCG vaccine induces a diverse range of immune processes including innate, cellular, humoral and non-specific or trained immunity [80]. These diverse and redundant immune processes likely make BCG vaccine-mediated protection more resilient to variations in clinical Mtb strain type which may explain our observations of similar levels of protection in the direct MGIA regardless of Mtb strain used. While reassuring that this was consistent between the *ex vivo* and *in vivo* models, future studies could include a wider range of clinical isolates with differential effect sizes for a more comprehensive validation, or evaluate immune protection induced by more targeted, subunit vaccine approaches which may be more sensitive to variation in Mtb strain type. The lack of a novel vaccine candidate proven to be superior to BCG is a notable challenge, with BCG providing the only current gold-standard for proof-of-concept in assay development and validation.

In the current study, the addition of flow cytometry and RNA-seq analysis to the MGIA workflow demonstrates the value of evaluating vaccine-induced mycobacterial control in combination with identification of correlates of growth inhibition. In the future this method may facilitate early, more informative evaluation of mycobacterial strains at clinical sites, generating insight into potential variations in vaccine-mediated protection from TB, as well as accelerating the identification of underlying immune mechanisms of protection.

In this study, three Mtb clinical isolates were evaluated using the *ex vivo* murine lung and spleen MGIA. We demonstrate that *ex vivo* growth inhibition of two selected isolates recapitulates vaccine-mediated CFU reduction in the lung and spleen following experimental Mtb infection in the mouse model. BCG-mediated protection against all three isolates selected for the study was observed at similar levels in the *ex vivo* MGIA and experimental Mtb infection. To conclude whether the MGIA can accurately recapitulate protection observed following experimental infection, further studies should include vaccine regimens known to demonstrate reduced efficacy against specific clinical isolates. Further, we analysed the host cell composition and transcriptome of cells preparations used in the MGIA and show that *ex vivo* BCG-mediated growth inhibition is associated with innate and adaptive immune mechanisms predominantly driven by myeloid cells, NK cells and IFNγ. Mtb lineage-specific correlates of growth inhibition were also identified and warrant further validation and investigation.

There is growing interest in the expansion of TB vaccine testing beyond standard laboratory strains of Mtb, with recommendations that vaccine candidates should be tested against multiple clinical strains. Currently, limited resources within the TB research field, and an emphasis on reducing, refining and replacing animal techniques, render *in vivo* studies an unsuitable tool to routinely test vaccines against an extended panel of strains. The *ex vivo* MGIA may represent a platform to gain early insight into vaccine performance against a collection of Mtb strains, alongside evaluation of correlates of growth inhibition.

Declaration of competing interest

The authors declare no competing interests.

Funding

This work was supported by a UK Medical Research Council studentship for HP (MR/N013638/1) and Rosetrees Trust grant A1256 for HP/HF/AZ. The funder played no role in study design, data collection, analysis and interpretation of data, or the writing of this manuscript. RT is a Jenner Investigator.

Data availability

RNA-seq datasets have been deposited in the NCBI GEO database

under accession numbers GSE224467 and GSE224469. All other datasets generated and analysed during the current study are available from the corresponding author on reasonable request.

CRediT authorship contribution statement

Hannah Painter: Writing – review & editing, Writing – original draft, Methodology, Investigation, Funding acquisition, Formal analysis. **Sam Willcocks:** Writing – review & editing, Investigation. **Andrea Zelmer:** Writing – review & editing, Supervision, Investigation, Funding acquisition, Conceptualization. **Rajko Reljic:** Writing – review & editing, Supervision, Funding acquisition, Conceptualization. **Rachel Tanner:** Writing – review & editing, Writing – original draft. **Helen Fletcher:** Writing – review & editing, Supervision, Funding acquisition, Conceptualization.

Acknowledgements

The authors are grateful to Nathalie Cadieux and Megan Fitzpatrick (Aeras) for provision of the BCG stocks, and Sebastian Gagneux (Swiss Tropical and Public Health Institute) for provision of the clinical isolate collection. The authors thank Sasha Larsen and Rhea Coler (Seattle Children's Research Institute) for helpful discussion of the project.

Appendix A. Supplementary data

Supplementary data to this article can be found online at https://doi.org/10.1016/j.tube.2024.102494.

References

[1] World Health Organization. Global tuberculosis report. 2022.
[2] Henao-Tamayo M, Shanley CA, Verma D, Zilavy A, Stapleton MC, Furney SK, Podell B, Orme IM. The efficacy of the BCG vaccine against newly emerging clinical strains of Mycobacterium tuberculosis. PLoS One 2015;10:e0136500. https://doi.org/10.1371/journal.pone.0136500.
[3] McShane H, Williams A. A review of preclinical animal models utilised for TB vaccine evaluation in the context of recent human efficacy data. Tuberculosis 2014;94:105–10. https://doi.org/10.1016/j.tube.2013.11.003.
[4] Borrell S, Trauner A, Brites D, Rigouts L, Loiseau C, Coscolla M, Niemann S, De Jong B, Yeboah-Manu D, Kato-Maeda M, Feldmann J, Reinhard M, Beisel C, Gagneux S. Reference set of Mycobacterium tuberculosis clinical strains: a tool for research and product development. PLoS One 2019;14:e0214088. https://doi.org/10.1371/journal.pone.0214088.
[5] Coscolla M, Gagneux S. Consequences of genomic diversity in Mycobacterium tuberculosis. Semin Immunol 2014;26:431–44. https://doi.org/10.1016/j.smim.2014.09.012.
[6] Coscolla M, Gagneux S, Menardo F, Loiseau C, Ruiz-Rodriguez P, Borrell S, Otchere ID, Asante-Poku A, Asare P, Sanchez-Buso L, Gehre F, Sanoussi CN, Antonio M, Affolabi D, Fyfe J, Beckert P, Niemann S, Alabi AS, Grobusch MP, Kobbe R, Parkhill J, Beisel C, Fenner L, Bottger EC, Meehan CJ, Harris SR, de Jong BC, Yeboah-Manu D, Brites D. Phylogenomics of Mycobacterium africanum reveals a new lineage and a complex evolutionary history. Microb Genom 2021;7. https://doi.org/10.1099/mgen.0.000477.
[7] Ngabonziza JCS, Loiseau C, Marceau M, Jouet A, Menardo F, Tzfadia O, Antoine R, Niyigena EB, Mulders W, Fissette K, Diels M, Gaudin C, Duthoy S, Ssengooba W, Andre E, Kaswa MK, Habimana YM, Brites D, Affolabi D, Mazarati JB, de Jong BC, Rigouts L, Gagneux S, Meehan CJ, Supply P. A sister lineage of the Mycobacterium tuberculosis complex discovered in the African Great Lakes region. Nat Commun 2020;11:2917. https://doi.org/10.1038/s41467-020-16626-6.
[8] Banaei-Esfahani S, Trauner A, Borrell S, Gygli SM, Rustad T, Feldmann J, Gillet L, Schubert OT, Sherman DR, Beisel C, Gagneux S, Aebersold R, Collins BC. Network analysis identifies regulators of lineage-specific phenotypes in Mycobacterium tuberculosis. *bioRxiv*. 2020. https://doi.org/10.1101/2020.02.14.943365.
[9] Chiner-Oms A, Berney M, Boinett C, Gonzalez-Candelas F, Young DB, Gagneux S, Jacobs Jr WR, Parkhill J, Cortes T, Comas I. Genome-wide mutational biases fuel transcriptional diversity in the Mycobacterium tuberculosis complex. Nat Commun 2019;10:3994. https://doi.org/10.1038/s41467-019-11948-6.
[10] Leisching G, Pietersen RD, van Heerden C, van Helden P, Wiid I, Baker B. RNAseq reveals hypervirulence-specific host responses to M. tuberculosis infection. Virulence 2017;8:848–58. https://doi.org/10.1080/21505594.2016.1250994.
[11] Ofori-Anyinam B, Riley AJ, Jobarteh T, Gitteh E, Sarr B, Faal-Jawara TI, Rigouts L, Senghore M, Kehinde A, Onyejepu N, Antonio M, de Jong BC, Gehre F, Meehan CJ. Comparative genomics shows differences in the electron transport and carbon metabolic pathways of Mycobacterium africanum relative to Mycobacterium tuberculosis and suggests an adaptation to low oxygen tension. Tuberculosis 2020;120:101899. https://doi.org/10.1016/j.tube.2020.101899.
[12] Rose G, Cortes T, Comas I, Coscolla M, Gagneux S, Young DB. Mapping of genotype-phenotype diversity among clinical isolates of mycobacterium tuberculosis by sequence-based transcriptional profiling. Genome Biol Evol 2013;5:1849–62. https://doi.org/10.1093/gbe/evt138.
[13] Sarkar R, Lenders L, Wilkinson KA, Wilkinson RJ, Nicol MP. Modern lineages of Mycobacterium tuberculosis exhibit lineage-specific patterns of growth and cytokine induction in human monocyte-derived macrophages. PLoS One 2012;7:e43170. https://doi.org/10.1371/journal.pone.0043170.
[14] Zhu L, Zhong J, Jia X, Liu G, Kang Y, Dong M, Zhang X, Li Q, Yue L, Li C, Fu J, Xiao J, Yan J, Zhang B, Lei M, Chen S, Lv L, Zhu B, Huang H, Chen F. Precision methylome characterization of Mycobacterium tuberculosis complex (MTBC) using PacBio single-molecule real-time (SMRT) technology. Nucleic Acids Res 2016;44:730–43. https://doi.org/10.1093/nar/gkv1498.
[15] Carpenter C, Sidney J, Kolla R, Nayak K, Tomiyama H, Tomiyama C, Padilla OA, Rozot V, Ahamed SF, Ponte C, Rolla V, Antas PR, Chandele A, Kenneth J, Laxmi S, Makgotlho E, Vanini V, Ippolito G, Kazanova AS, Panteleev AV, Hanekom W, Mayanja-Kizza H, Lewinsohn D, Saito M, McElrath MJ, Boom WH, Goletti D, Gilman R, Lyadova IV, Scriba TJ, Kallas EG, Murali-Krishna K, Sette A, Lindestam Arlehamn CS. A side-by-side comparison of T cell reactivity to fifty-nine Mycobacterium tuberculosis antigens in diverse populations from five continents. Tuberculosis 2015;95:713–21. https://doi.org/10.1016/j.tube.2015.07.001.
[16] Flesch I, Kaufmann SH. Mycobacterial growth inhibition by interferon-gamma-activated bone marrow macrophages and differential susceptibility among strains of Mycobacterium tuberculosis. J Immunol 1987;138:4408–13.
[17] Krishnan N, Malaga W, Constant P, Caws M, Tran TH, Salmons J, Nguyen TN, Nguyen DB, Daffe M, Young DB, Robertson BD, Guilhot C, Thwaites GE. Mycobacterium tuberculosis lineage influences innate immune response and virulence and is associated with distinct cell envelope lipid profiles. PLoS One 2011;6:e23870. https://doi.org/10.1371/journal.pone.0023870.
[18] Mourik BC, de Steenwinkel JEM, de Knegt GJ, Huizinga R, Verbon A, Ottenhoff THM, van Soolingen D, Leenen PJM. Mycobacterium tuberculosis clinical isolates of the Beijing and East-African Indian lineage induce fundamentally different host responses in mice compared to H37Rv. Sci Rep 2019;9:19922. https://doi.org/10.1038/s41598-019-56300-6.
[19] Portevin D, Gagneux S, Comas I, Young D. Human macrophage responses to clinical isolates from the Mycobacterium tuberculosis complex discriminate between ancient and modern lineages. PLoS Pathog 2011;7:e1001307. https://doi.org/10.1371/journal.ppat.1001307.
[20] Reiling N, Homolka S, Walter K, Brandenburg J, Niwinski L, Ernst M, Herzmann C, Lange C, Diel R, Ehlers S, Niemann S. Clade-specific virulence patterns of Mycobacterium tuberculosis complex strains in human primary macrophages and aerogenically infected mice. mBio 2013;4. https://doi.org/10.1128/mBio.00250-13.
[21] Ribeiro SC, Gomes LL, Amaral EP, Andrade MR, Almeida FM, Rezende AL, Lanes VR, Carvalho EC, Suffys PN, Mokrousov I, Lasunskaia EB. Mycobacterium tuberculosis strains of the modern sublineage of the Beijing family are more likely to display increased virulence than strains of the ancient sublineage. J Clin Microbiol 2014;52:2615–24. https://doi.org/10.1128/JCM.00498-14.
[22] Tientcheu LD, Sutherland JS, de Jong BC, Kampmann B, Jafali J, Adetifa IM, Antonio M, Dockrell HM, Ota MO. Differences in T-cell responses between Mycobacterium tuberculosis and Mycobacterium africanum-infected patients. Eur J Immunol 2014;44:1387–98. https://doi.org/10.1002/eji.201343956.
[23] Tanner R, McShane H. Replacing, reducing and refining the use of animals in tuberculosis vaccine research. ALTEX 2017;34:157–66. https://doi.org/10.14573/altex.1607281.
[24] Jeon BY, Derrick SC, Lim J, Kolibab K, Dheenadhayalan V, Yang AL, Kreiswirth B, Morris SL. Mycobacterium bovis BCG immunization induces protective immunity against nine different Mycobacterium tuberculosis strains in mice. Infect Immun 2008;76:5173–80. https://doi.org/10.1128/IAI.00019-08.
[25] Levillain F, Kim H, Woong Kwon K, Clark S, Cia F, Malaga W, Lanni F, Brodin P, Gicquel B, Guilhot C, Bancroft GJ, Williams A, Jae Shin S, Poquet Y, Neyrolles O. Preclinical assessment of a new live attenuated Mycobacterium tuberculosis Beijing-based vaccine for tuberculosis. Vaccine 2020;38:1416–23. https://doi.org/10.1016/j.vaccine.2019.11.085.
[26] Lopez B, Aguilar D, Orozco H, Burger M, Espitia C, Ritacco V, Barrera L, Kremer K, Hernandez-Pando R, Huygen K, van Soolingen D. A marked difference in pathogenesis and immune response induced by different Mycobacterium tuberculosis genotypes. Clin Exp Immunol 2003;133:30–7. https://doi.org/10.1046/j.1365-2249.2003.02171.x.
[27] Ordway DJ, Shang S, Henao-Tamayo M, Obregon-Henao A, Nold L, Caraway M, Shanley CA, Basaraba RJ, Duncan CG, Orme IM. Mycobacterium bovis BCG-mediated protection against W-Beijing strains of Mycobacterium tuberculosis is diminished concomitant with the emergence of regulatory T cells. Clin Vaccine Immunol 2011;18:1527–35. https://doi.org/10.1128/CVI.05127-11.
[28] Perez I, Uranga S, Sayes F, Frigui W, Samper S, Arbues A, Aguilo N, Brosch R, Martin C, Gonzalo-Asensio J. Live attenuated TB vaccines representing the three modern Mycobacterium tuberculosis lineages reveal that the Euro-American genetic background confers optimal vaccine potential. EBioMedicine 2020;55:102761. https://doi.org/10.1016/j.ebiom.2020.102761.
[29] Tsenova L, Harbacheuski R, Sung N, Ellison E, Fallows D, Kaplan G. BCG vaccination confers poor protection against M. tuberculosis HN878-induced central nervous system disease. Vaccine 2007;25:5126–32. https://doi.org/10.1016/j.vaccine.2006.11.024.
[30] Tanner R, O'Shea MK, Fletcher HA, McShane H. In vitro mycobacterial growth inhibition assays: a tool for the assessment of protective immunity and evaluation

of tuberculosis vaccine efficacy. Vaccine 2016;34:4656–65. https://doi.org/10.1016/j.vaccine.2016.07.058.
[31] Basu Roy R, Sambou B, Sissoko M, Holder B, Gomez MP, Egere U, Sillah AK, Koukounari A, Kampmann B. Protection against mycobacterial infection: a case-control study of mycobacterial immune responses in pairs of Gambian children with discordant infection status despite matched TB exposure. EBioMedicine 2020;59:102891. https://doi.org/10.1016/j.ebiom.2020.102891.
[32] Denis M, Wedlock DN, Buddle BM. Ability of T cell subsets and their soluble mediators to modulate the replication of Mycobacterium bovis in bovine macrophages. Cell Immunol 2004;232:1–8. https://doi.org/10.1016/j.cellimm.2005.01.003.
[33] Dijkman K, Vervenne RAW, Sombroek CC, Boot C, Hofman SO, van Meijgaarden KE, Ottenhoff THM, Kocken CHM, Haanstra KG, Vierboom MPM, Verreck FAW. Disparate tuberculosis disease development in macaque species is associated with innate immunity. Front Immunol 2019;10:2479. https://doi.org/10.3389/fimmu.2019.02479.
[34] Painter H, Prabowo SA, Cia F, Stockdale L, Tanner R, Willcocks S, Reljic R, Fletcher HA, Zelmer A. Adaption of the ex vivo mycobacterial growth inhibition assay for use with murine lung cells. Sci Rep 2020;10:3311. https://doi.org/10.1038/s41598-020-60223-y.
[35] Tanner R, Satti I, Harris SA, O'Shea MK, Cizmeci D, O'Connor D, Chomka A, Matsumiya M, Wittenberg R, Minassian AM, Meyer J, Fletcher HA, McShane H. Tools for assessing the protective efficacy of TB vaccines in humans: in vitro mycobacterial growth inhibition predicts outcome of in vivo mycobacterial infection. Front Immunol 2019;10:2983. https://doi.org/10.3389/fimmu.2019.02983.
[36] Tanner R, White AD, Boot C, Sombroek CC, O'Shea MK, Wright D, Hoogkamer E, Bitencourt J, Harris SA, Sarfas C, Wittenberg R, Satti I, Fletcher HA, Verreck FAW, Sharpe SA, McShane H. A non-human primate in vitro functional assay for the early evaluation of TB vaccine candidates. NPJ Vaccines 2021;6:3. https://doi.org/10.1038/s41541-020-00263-7.
[37] Zelmer A, Tanner R, Stylianou E, Damelang T, Morris S, Izzo A, Williams A, Sharpe S, Pepponi I, Walker B, Hokey DA, McShane H, Brennan M, Fletcher H. A new tool for tuberculosis vaccine screening: ex vivo Mycobacterial Growth Inhibition Assay indicates BCG-mediated protection in a murine model of tuberculosis. BMC Infect Dis 2016;16:412. https://doi.org/10.1186/s12879-016-1751-4.
[38] Marsay L, Matsumiya M, Tanner R, Poyntz H, Griffiths KL, Stylianou E, Marsh PD, Williams A, Sharpe S, Fletcher H, McShane H. Mycobacterial growth inhibition in murine splenocytes as a surrogate for protection against Mycobacterium tuberculosis (M. tb). Tuberculosis 2013;93:551–7. https://doi.org/10.1016/j.tube.2013.04.007.
[39] Parra M, Yang AL, Lim J, Kolibab K, Derrick S, Cadieux N, Perera LP, Jacobs WR, Brennan M, Morris SL. Development of a murine mycobacterial growth inhibition assay for evaluating vaccines against Mycobacterium tuberculosis. Clin Vaccine Immunol 2009;16:1025–32. https://doi.org/10.1128/CVI.00067-09.
[40] Yang AL, Schmidt TE, Stibitz S, Derrick SC, Morris SL, Parra M. A simplified mycobacterial growth inhibition assay (MGIA) using direct infection of mouse splenocytes and the MGIT system. J Microbiol Methods 2016;131:7–9. https://doi.org/10.1016/j.mimet.2016.09.010.
[41] Kilkenny C, Browne WJ, Cuthill IC, Emerson M, Altman DG. Improving bioscience research reporting: the ARRIVE guidelines for reporting animal research. Animals 2014;4:35–44. https://doi.org/10.3390/ani4010035.
[42] Zelmer A, Tanner R, Stylianou E, Morris S, Izzo A, Williams A, Sharpe S, Pepponi I, Walker B, Hokey DA, McShane H, Brennan M, Fletcher H. Ex vivo mycobacterial growth inhibition assay (MGIA) for tuberculosis vaccine testing - a protocol for mouse splenocytes. bioRxiv 2015. https://doi.org/10.1101/020560.
[43] Misharin AV, Morales-Nebreda L, Mutlu GM, Budinger GR, Perlman H. Flow cytometric analysis of macrophages and dendritic cell subsets in the mouse lung. Am J Respir Cell Mol Biol 2013;49:503–10. https://doi.org/10.1165/rcmb.2013-0086MA.
[44] Yu YR, O'Koren EG, Hotten DF, Kan MJ, Kopin D, Nelson ER, Que L, Gunn MD. A protocol for the comprehensive flow cytometric analysis of immune cells in normal and inflamed murine non-lymphoid tissues. PLoS One 2016;11:e0150606. https://doi.org/10.1371/journal.pone.0150606.
[45] Bushnell B. BBTools. 2014. https://sourceforge.net/projects/bbmap/.
[46] Cunningham F, Achuthan P, Akanni W, Allen J, Amode MR, Armean IM, Bennett R, Bhai J, Billis K, Boddu S, Cummins C, Davidson C, Dodiya KJ, Gall A, Giron CG, Gil L, Grego T, Haggerty L, Haskell E, Hourlier T, Izuogu OG, Janacek SH, Juettemann T, Kay M, Laird MR, Lavidas I, Liu Z, Loveland JE, Marugan JC, Maurel T, McMahon AC, Moore B, Morales J, Mudge JM, Nuhn M, Ogeh D, Parker A, Parton A, Patricio M, Abdul Salam AI, Schmitt BM, Schuilenburg H, Sheppard D, Sparrow H, Stapleton E, Szuba M, Taylor K, Threadgold G, Thormann A, Vullo A, Walts B, Winterbottom A, Zadissa A, Chakiachvili M, Frankish A, Hunt SE, Kostadima M, Langridge N, Martin FJ, Muffato M, Perry E, Ruffier M, Staines DM, Trevanion SJ, Aken BL, Yates AD, Zerbino DR, Flicek P, Ensembl. Nucleic Acids Res 2019;47:D745–51. https://doi.org/10.1093/nar/gky1113. 2019.
[47] Dobin A, Davis CA, Schlesinger F, Drenkow J, Zaleski C, Jha S, Batut P, Chaisson M, Gingeras TR. STAR: ultrafast universal RNA-seq aligner. Bioinformatics 2013;29:15–21. https://doi.org/10.1093/bioinformatics/bts635.
[48] Shi W, Liao Y. Rsubread/subread users guide. 2023. https://bioconductor.org/packages/release/bioc/vignettes/Rsubread/inst/doc/SubreadUsersGuide.pdf.
[49] Andrews S. FastQC: a quality control tool for high throughput sequence data. 2023. http://www.bioinformatics.babraham.ac.uk/projects/fastqc/.
[50] Institute B. Picard tools. 2023. http://broadinstitute.github.io/picard/.
[51] Love MI, Huber W, Anders S. Moderated estimation of fold change and dispersion for RNA-seq data with DESeq2. Genome Biol 2014;15:550. https://doi.org/10.1186/s13059-014-0550-8.
[52] Benjamini Y, Hochberg Y. Controlling the false discovery rate: a practical and powerful approach to multiple testing. J Roy Stat Soc B 1995;57:289–300.
[53] Singhania A, Graham CM, Gabrysova L, Moreira-Teixeira L, Stavropoulos E, Pitt JM, Chakravarty P, Warnatsch A, Branchett WJ, Conejero L, Lin JW, Davidson S, Wilson MS, Bancroft G, Langhorne J, Frickel E, Sesay AK, Priestnall SL, Herbert E, Ioannou M, Wang Q, Humphreys IR, Dodd J, Openshaw PJM, Mayer-Barber KD, Jankovic D, Sher A, Lloyd CM, Baldwin N, Chaussabel D, Papayannopoulos V, Wack A, Banchereau JF, Pascual VM, O'Garra A. Transcriptional profiling unveils type I and II interferon networks in blood and tissues across diseases. Nat Commun 2019;10:2887. https://doi.org/10.1038/s41467-019-10601-6.
[54] Weiner 3rd J, Domaszewska T. tmod: an R package for general and multivariate enrichment analysis. PeerJ Preprints 2016. https://doi.org/10.7287/peerj.preprints.2420v1.
[55] Yamaguchi KD, Ruderman DL, Croze E, Wagner TC, Velichko S, Reder AT, Salamon H. IFN-beta-regulated genes show abnormal expression in therapy-naive relapsing-remitting MS mononuclear cells: gene expression analysis employing all reported protein-protein interactions. J Neuroimmunol 2008;195:116–20. https://doi.org/10.1016/j.jneuroim.2007.12.007.
[56] Barczak AK, Domenech P, Boshoff HI, Reed MB, Manca C, Kaplan G, Barry 3rd CE. In vivo phenotypic dominance in mouse mixed infections with Mycobacterium tuberculosis clinical isolates. J Infect Dis 2005;192:600–6. https://doi.org/10.1086/432006.
[57] Manabe YC, Dannenberg Jr AM, Tyagi SK, Hatem CL, Yoder M, Woolwine SC, Zook BC, Pitt ML, Bishai WR. Different strains of Mycobacterium tuberculosis cause various spectrums of disease in the rabbit model of tuberculosis. Infect Immun 2003;71:6004–11. https://doi.org/10.1128/IAI.71.10.6004-6011.2003.
[58] Marquina-Castillo B, Garcia-Garcia L, Ponce-de-Leon A, Jimenez-Corona ME, Bobadilla-Del Valle M, Cano-Arellano B, Canizales-Quintero S, Martinez-Gamboa A, Kato-Maeda M, Robertson B, Young D, Small P, Schoolnik G, Sifuentes-Osornio J, Hernandez-Pando R. Virulence, immunopathology and transmissibility of selected strains of Mycobacterium tuberculosis in a murine model. Immunology 2009;128:123–33. https://doi.org/10.1111/j.1365-2567.2008.03004.x.
[59] Palanisamy GS, DuTeau N, Eisenach KD, Cave DM, Theus SA, Kreiswirth BN, Basaraba RJ, Orme IM. Clinical strains of Mycobacterium tuberculosis display a wide range of virulence in Guinea pigs. Tuberculosis 2009;89:203–9. https://doi.org/10.1016/j.tube.2009.01.005.
[60] Romagnoli A, Petruccioli E, Palucci I, Camassa S, Carata E, Petrone L, Mariano S, Sali M, Dini L, Girardi E, Delogu G, Goletti D, Fimia GM. Clinical isolates of the modern Mycobacterium tuberculosis lineage 4 evade host defense in human macrophages through eluding IL-1beta-induced autophagy. Cell Death Dis 2018;9:624. https://doi.org/10.1038/s41419-018-0640-8.
[61] Kaveh DA, Bachy VS, Hewinson RG, Hogarth PJ. Systemic BCG immunization induces persistent lung mucosal multifunctional CD4 T(EM) cells which expand following virulent mycobacterial challenge. PLoS One 2011;6:e21566. https://doi.org/10.1371/journal.pone.0021566.
[62] Rook GA, Champion BR, Steele J, Varey AM, Stanford JL. I-A restricted activation by T cell lines of anti-tuberculosis activity in murine macrophages. Clin Exp Immunol 1985;59:414–20.
[63] Steele J, Flint KC, Pozniak AL, Hudspith B, Johnson MM, Rook GA. Inhibition of virulent Mycobacterium tuberculosis by murine peritoneal macrophages and human alveolar lavage cells: the effects of lymphokines and recombinant gamma interferon. Tubercle 1986;67:289–94. https://doi.org/10.1016/0041-3879(86)90018-8.
[64] Kaveh DA, Garcia-Pelayo MC, Hogarth PJ. Persistent BCG bacilli perpetuate CD4 T effector memory and optimal protection against tuberculosis. Vaccine 2014;32:6911–8. https://doi.org/10.1016/j.vaccine.2014.10.041.
[65] Zelmer A, Stockdale L, Prabowo SA, Cia F, Spink N, Gibb M, Eddaoudi A, Fletcher HA. High monocyte to lymphocyte ratio is associated with impaired protection after subcutaneous administration of BCG in a mouse model of tuberculosis. F1000Res 2018;7:296. https://doi.org/10.12688/f1000research.14239.2.
[66] Huang L, Nazarova EV, Tan S, Liu Y, Russell DG. Growth of Mycobacterium tuberculosis in vivo segregates with host macrophage metabolism and ontogeny. J Exp Med 2018;215:1135–52. https://doi.org/10.1084/jem.20172020.
[67] Dhiman R, Periasamy S, Barnes PF, Jaiswal AG, Paidipally P, Barnes AB, Tvinnereim A, Vankayalapati R. NK1.1+ cells and IL-22 regulate vaccine-induced protective immunity against challenge with Mycobacterium tuberculosis. J Immunol 2012;189:897–905. https://doi.org/10.4049/jimmunol.1102833.
[68] Aranday Cortes E, Kaveh D, Nunez-Garcia J, Hogarth PJ, Vordermeier HM. Mycobacterium bovis-BCG vaccination induces specific pulmonary transcriptome biosignatures in mice. PLoS One 2010;5:e11319. https://doi.org/10.1371/journal.pone.0011319.
[69] Irwin SM, Goodyear A, Keyser A, Christensen R, Troudt JM, Taylor JL, Bohsali A, Briken V, Izzo AA. Immune response induced by three Mycobacterium bovis BCG substrains with diverse regions of deletion in a C57BL/6 mouse model. Clin Vaccine Immunol 2008;15:750–6. https://doi.org/10.1128/CVI.00018-08.
[70] Dorhoi A, Yeremeev V, Nouailles G, Weiner 3rd J, Jorg S, Heinemann E, Oberbeck-Muller D, Knaul JK, Vogelzang A, Reece ST, Hahnke K, Mollenkopf HJ, Brinkmann V, Kaufmann SH. Type I IFN signaling triggers immunopathology in tuberculosis-susceptible mice by modulating lung phagocyte dynamics. Eur J Immunol 2014;44:2380–93. https://doi.org/10.1002/eji.201344219.

[71] Manca C, Tsenova L, Freeman S, Barczak AK, Tovey M, Murray PJ, Barry C, Kaplan G. Hypervirulent M. tuberculosis W/Beijing strains upregulate type I IFNs and increase expression of negative regulators of the Jak-Stat pathway. J Interferon Cytokine Res 2005;25:694–701. https://doi.org/10.1089/jir.2005.25.694.

[72] Mayer-Barber KD, Andrade BB, Oland SD, Amaral EP, Barber DL, Gonzales J, Derrick SC, Shi R, Kumar NP, Wei W, Yuan X, Zhang G, Cai Y, Babu S, Catalfamo M, Salazar AM, Via LE, Barry 3rd CE, Sher A. Host-directed therapy of tuberculosis based on interleukin-1 and type I interferon crosstalk. Nature 2014;511:99–103. https://doi.org/10.1038/nature13489.

[73] Moreira-Teixeira L, Mayer-Barber K, Sher A, O'Garra A. Type I interferons in tuberculosis: foe and occasionally friend. J Exp Med 2018;215:1273–85. https://doi.org/10.1084/jem.20180325.

[74] Zhang G, deWeerd NA, Stifter SA, Liu L, Zhou B, Wang W, Zhou Y, Ying B, Hu X, Matthews AY, Ellis M, Triccas JA, Hertzog PJ, Britton WJ, Chen X, Feng CG. A proline deletion in IFNAR1 impairs IFN-signaling and underlies increased resistance to tuberculosis in humans. Nat Commun 2018;9:85. https://doi.org/10.1038/s41467-017-02611-z.

[75] Denis M. Recombinant murine beta interferon enhances resistance of mice to systemic Mycobacterium avium infection. Infect Immun 1991;59:1857–9. https://doi.org/10.1128/iai.59.5.1857-1859.1991.

[76] Donovan ML, Schultz TE, Duke TJ, Blumenthal A. Type I interferons in the pathogenesis of tuberculosis: molecular drivers and immunological consequences. Front Immunol 2017;8:1633. https://doi.org/10.3389/fimmu.2017.01633.

[77] Kuchtey J, Fulton SA, Reba SM, Harding CV, Boom WH. Interferon-alphabeta mediates partial control of early pulmonary Mycobacterium bovis bacillus Calmette-Guerin infection. Immunology 2006;118:39–49. https://doi.org/10.1111/j.1365-2567.2006.02337.x.

[78] Mai D, Jahn A, Murray T, Morikubo M, Nemeth J, Urdahl K, Diercks AH, Aderem A, Rothchild AC. Mycobacterial exposure remodels alveolar macrophages and the early innate response to Mycobacterium tuberculosis infection. bioRxiv 2022. https://doi.org/10.1101/2022.09.19.507309.

[79] Gopal R, Monin L, Slight S, Uche U, Blanchard E, Fallert Junecko BA, Ramos-Payan R, Stallings CL, Reinhart TA, Kolls JK, Kaushal D, Nagarajan U, Rangel-Moreno J, Khader SA. Unexpected role for IL-17 in protective immunity against hypervirulent Mycobacterium tuberculosis HN878 infection. PLoS Pathog 2014;10:e1004099. https://doi.org/10.1371/journal.ppat.1004099.

[80] Li J, Zhan L, Qin C. The double-sided effects of Mycobacterium Bovis bacillus Calmette-Guerin vaccine. NPJ Vaccines 2021;6:14. https://doi.org/10.1038/s41541-020-00278-0.